

Chapter

Casting Techniques: An Alternative for Producing Parts with Recycled Al in the Gravity Die Casting Process

Narducci Carlos Jr.

Abstract

This work applied the grain refinement technique by heterogeneous nucleation and precipitation hardening to investigate the effect of size and morphology of β -Fe particles on Al-Si alloys' mechanical behavior Fe-critical, inoculated via Nb+B and heat-treated. The samples for the microstructural analyses were produced according to the standard mold, Test Procedure-1 (TP-1) and, analyzed by optical microscope with polarised light and filter plate and differential interference contrast (DIC) and by X-ray energy dispersive spectroscopy (XRD SEM) with EDS detector analyzer. The specimens for the mechanical tests were cast in a metal mold according to ASTM B108. The combined effect of manipulating the studied alloy Al10Si1Fe0.35Mg resulted in reduced and spheroidized β -Fe precipitates with improved mechanical properties in the material. Properties are similar to those achieved by commercially used alloys with engineering applications in structural and safety parts.

Keywords: recycled Al, Al-Si, Nb + B, casting, heat treatment, mechanical properties, grain refinement, and intermetallic precipitates

1. Introduction

The increasing need for weight reduction in means of transport has made Aluminum (Al) one of the main consumer materials in the world. Another benefit of Al is its capacity to be recycled infinite times without losing its properties. Aluminum recycling is a way of reusing the material used, transforming it into new products for consumption. Its contribution in reducing the energy spent in its production and favor of the environment has become an urgent issue, of all, with a consensus that the use of the planet's resources must be sustainably [1, 2].

However, recycled Al is still restricted for structural and safety products due to the percentage of Fe-critical contained in Al alloys coming from recycling.

The Fe-critical precipitates the formation of coarse particles of β -Al₅FeSi (β -Fe), which weaken the material, impairing its mechanical properties [3]. Therefore, in the search for a new perspective for the use of recycled Al in gravity die casting processes for the production of structural and safety parts and components, this work studies the creation of a strengthening mechanism in the structure of the material through the manipulation of the intermetallic precipitates of β -Fe by the heterogeneous nucleation phenomenon, through the addition of the inoculant via niobium (Nb) and boron (B) and, the addition of the element magnesium (Mg), to cause precipitation hardening. The simultaneous use of the two techniques results in improvements to the material's mechanical properties.

Figure 1 shows some examples of products with automotive applications that can benefit from this process: Master Cylinders, Tweezers, camshaft rocker arms, and suspension bracket components, among other automotive and aerospace components.

1.1 Nucleation

From classical nucleation theory, we know that nucleation of a particle can occur in a homogeneous or heterogeneous manner, with the formation of nuclei that can form an embryo and eventually be able to grow, depending on the temperature or variation of the free energy of the system [4–7]. An understanding of homogeneous nucleation will help us to understand heterogeneous nucleation better. In homogeneous nucleation, there is no interface in the system and occurs when there is a grouping of solute atoms in the matrix so that the radius of the particle embryo exceeds a certain radius value, known as the critical radius (r^*), for the formation of a stable nucleus, given a certain temperature fluctuation. Solid nuclei emerge from the liquid. The embryo becomes a stable nucleus from the nucleation process which is energetically activated when the particle exceeds the critical radius, representing the free energy peak (ΔG). **Figure 2** brings a schematic representation of the homogeneous nucleation process.



Figure 1. Customers and automotive products with the potential use of the techniques.

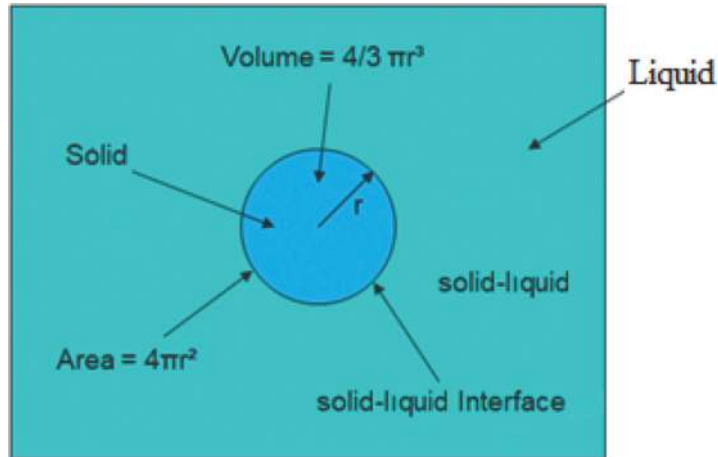


Figure 2.
 Schematic illustration of the homogeneous nucleation particle, adapted from [7].

The theory is based on the free energy between the liquid and solid interfaces. The highest free energy for homogeneous nucleation to occur (ΔG^*_{hom}) can be expressed as shown in Eq. (1) [4]:

$$\Delta G^*_{\text{hom}} = -V \Delta G_v + A \gamma_{SL} \quad (1)$$

Where: V is the volume of the sphere, ΔG is the variation of the free energy of the system, A is the area of the sphere, and γ_{SL} is the surface tension between the solid and the liquid [4].

For heterogeneous nucleation, there must be an interface (particles of other elements, impurities, etc.), a phenomenon that decreases the variation of free energy for forming an embryo. Therefore the nucleation will be considered heterogeneous when it takes place on the surface of the mold or of the particles present in the system. The theory was developed by [8]. The critical factor is the wetting angle (θ), which occurs as a function of the interface energy of the mold surface γ_{SL} , the crystal-substrate interface γ_{SM} , and the liquid-substrate interface γ_{ML} , as shown in **Figure 3**. The wetting angle θ can be calculated as shown in Eq. (2) [8]:

$$\cos \theta = (\gamma_{ML} - \gamma_{SM}) / \gamma_{SL} \quad (2)$$

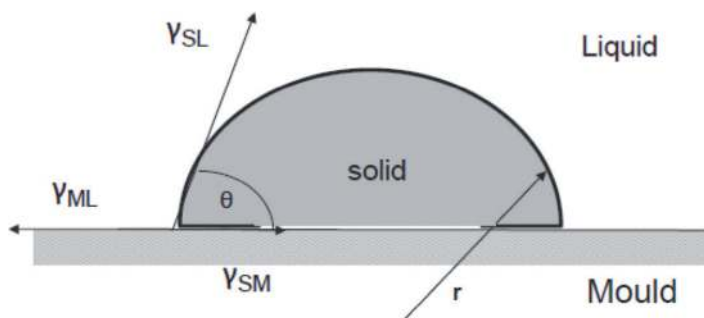


Figure 3.
 Schematic illustration of the wetting angle between the mold and the solid, adapted from [7].

One of the most important technical aspects of casting is the control of nucleation grain size and shape, together with the segregation effects that occur during casting, which can significantly influence the physical and mechanical properties of the cast product. Most commonly, control is exercised by the use of nucleating agents (inoculants). With this, the growth of grains occurs simultaneously with the nucleation of other grains in different parts of the liquid. The competition between nucleation and grain growth will determine the final macrostructure (grain refinement), which gives the product its mechanical properties.

After nucleation, the first step to be considered is grain growth. The grain growth depends on the nature of the interface between the wetting, the solid, and the liquid. The structure and shape of the interface influence both the morphology and size of the grains and the number and distribution of imperfections in the solid. The solidification can occur in planar, cellular, or dendritic form [9].

In Al alloys, grain growth is dendritic [10]. Suppose a state of metastability or instability is created near the growth interface by the occurrence of an inverted gradient of free energy. In that case, the growth energy will break and grow laterally and develop lateral ramifications, according to **Figure 4**.

Scientists developed the grain refinement theory from observations with Al-Ti-B additions in Al alloys. Currently, two strands are used to explain these phenomena; (a) the nucleating paradigm with the nucleating particle theory and phase diagram theory and (b) the solute paradigm theory [12, 13]. The schematic presentation in **Figure 5** brings the proposal presented for the theories.

With the knowledge of grain refinement, the studies will delve into manipulating the available parameters to obtain the best result of grain refinement. With this, the element Nb emerged [14–17].

1.2 Precipitation hardening

Precipitation hardening is a technique used in Al-Si cast alloys, usually with a Fe content within recommended limits (e.g., ASTM A357 alloy), to strengthen the mechanical properties of the material. The process consists of adding a precipitating

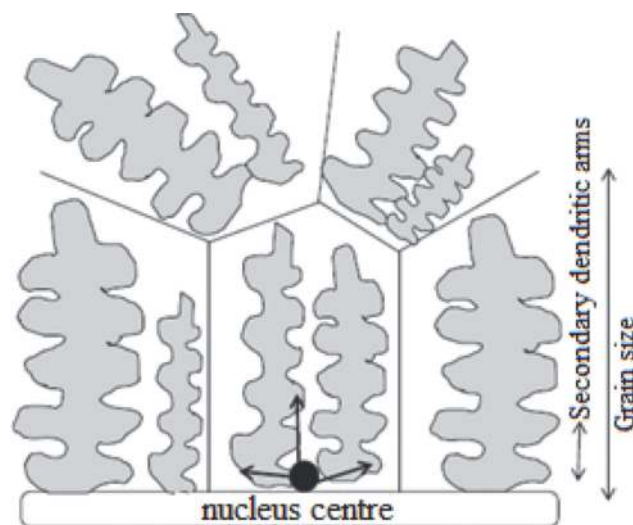


Figure 4. Schematic illustration of dendritic grain growth, adapted from [11].

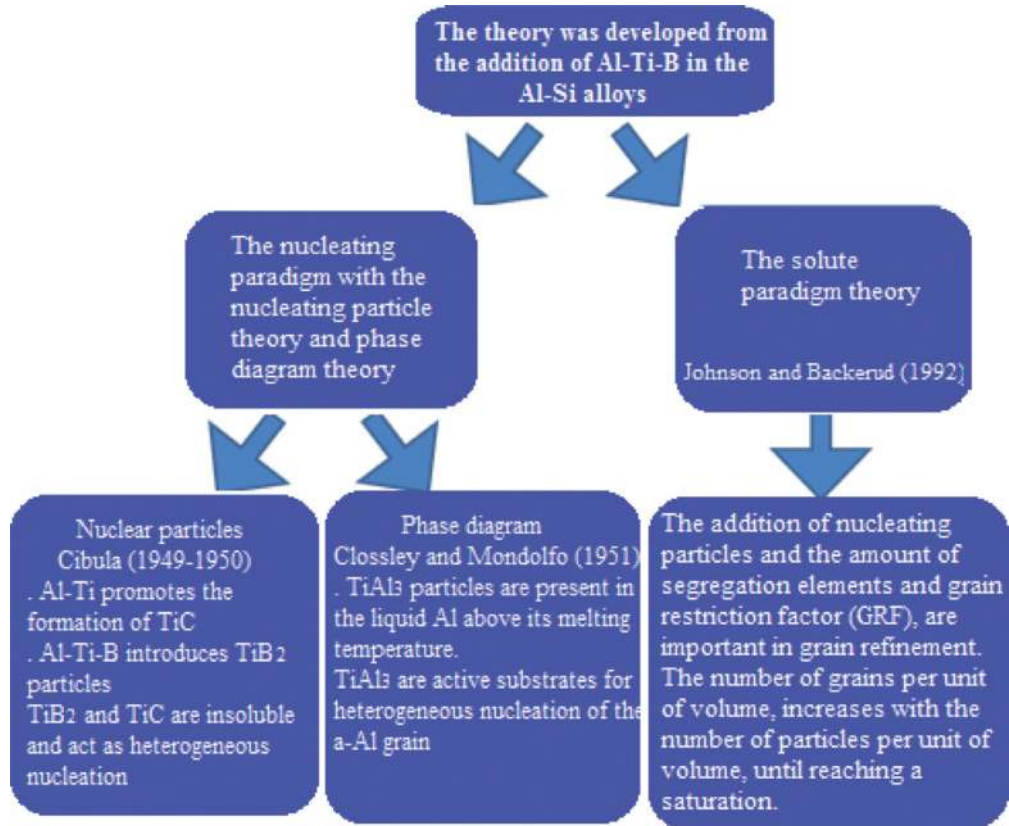


Figure 5. Schematic presentation of the theories: Nucleating particles, phase diagram and solute paradigm [12, 13].

alloying element, such as Mg or Cu, to the material, with subsequent solubilization and precipitation heat treatment (T6). During the heat treatment, the material is heated within the single-phase region for a sufficient time to solubilize the solute atoms, followed by rapid cooling to obtain a supersaturated solid solution. Subsequently, the alloy is reheated to a temperature below the single-phase region to allow the precipitation of finely dispersed particles from the supersaturated solid solution. The formation of a dispersion of fine precipitates hinders the movement of the dislocations [7, 18–21].

Heat treatment is one of the mechanisms that, through phase transformation, can change the microstructure of the material, giving it a set of desirable mechanical characteristics. The heat treatment route is carried out, having as basis the phase diagram, in a convenient way to achieve some of these desired transformations, related to time and temperature, to find the ideal processing parameters for a given alloy. Most phase transformations depend on the reaction progress as a function of time or the transformation rate involving solid phases. A new phase is formed during transformations, with different physical and chemical characteristics from those of the phase that gave rise to it. Normally, the formation of new phases begins by forming small nuclei with subsequent growth. The growth will continue until the equilibrium condition is reached. This heat treatment, applied to Al alloys, is known as precipitation hardening because the small particles of the new phase are known as “precipitates.” The denomination “age hardening” is also used to designate this procedure because the resistance develops over time. **Figure 6** helps to understand the mechanism of the transformations [7, 22].

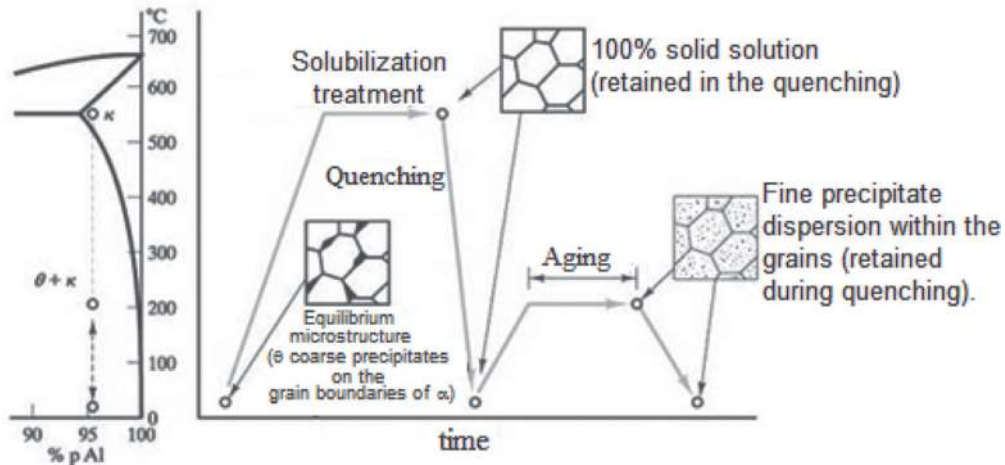


Figure 6.

Heating up to solubilization temperature, rapid cooling (quenching), and then reheating below solubilization temperature (aging). With this, a fine dispersion of precipitates is formed within the grains, adapted from [22].

Al-Si alloys, with the addition of some more elements, such as Mg or Cu, are heat-treatable alloys, i.e., they can have their mechanical strength increased by appropriate heat treatment. The mechanical properties of Al-Si alloys depend on the morphology and distribution of the eutectic second phase particles. The brittleness of the coarse, second phase fibers is the main reason for low elasticity and low tensile and impact strengths. However, the fine, dispersed, and globular second phase particles, combined with precipitates formed during the aging process, can result in excellent mechanical properties. Significant improvements in the mechanical properties of alloys, especially elasticity, can be obtained with solubilization and aging treatment, which changes the morphology and distribution of the precipitated particles. Previous studies show that alloys aged with high silicon content, above 5%, have better mechanical properties than alloys with low silicon content [23]. The choice of the element used for precipitation in Al-Si alloy in this work was Mg.

2. Experimental procedures

2.1 Casting

The materials used were: Primary Al (supplied by HYDRO), Si (supplied by LIASA), Fe (supplied by MEXTRAMETAL), and Al4Nb0.05B master alloy (supplied by Companhia Brasileira de Metalurgia e Mineração - CBMM). The casting materials (supplied by ALFA TREND).

Four types of specimens (CDPs) were produced, from the Al10Si1Fe alloy: without and with the addition of the inoculant NbB, to allow the evaluation of the influence of grain refinement on the morphology of the β -Fe precipitates; and, without and with the addition of the element Mg, to enable the evaluation of the aging potential by precipitation of the alloy with the introduction of this element. **Table 1** presents the chemical composition of each batch produced.

The CDPs were produced at the Foundry (Sunny in SP-Itaquaquecetuba). The metal melting was in an electric crucible furnace, with a capacity of 60 kg of material.

Batch	Elements (Wt. %)					
	Al	Si	Fe	Nb	B	Mg
1°	balance	10	1	0	0	0
2°	balance	10	1	0,05	0,00625	0
3°	balance	10	1	0,05	0,00625	0,35
4°	balance	10	1	0	0	0,35

Table 1.
Chemical composition of the CDPs.

After adding each element, the temperature was stabilized at $850 \pm 10^\circ\text{C}$, a retention of 1 hour was applied to ensure complete dissolution. Degassing was then performed by the addition of hexachloroethane tablets. At each sample, collection homogenization was achieved by 30 s of manual stirring and a further stabilization in temperature at $720 \pm 10^\circ\text{C}$, followed by a second homogenization at the same temperature, with 30 s of stirring and sampling. The verification of the base alloy was by atomic absorption spectrometry.

Figure 7 shows the casting, through the gravity die casting process, using a 1020 steel metal mold manufactured according to ASTM B108 (supplied by Alpha Trend). The mold construction followed the international standard, enabling comparisons with other studies and research results. The mold was built in two halves and two cavities, producing two CDPs per pour. The mold feeding system was made with a central filling channel that distributes the metal in two auxiliary side feeding channels, making the liquid metal feed the product from bottom to top and through two inlet channels in each part. This system minimizes the material turbulence during the part filling. Before pouring the liquid metal, the mold was painted with water-based graphite paint and heated with a blowtorch to a temperature of 250°C .

2.2 Microscopic analysis

Figure 8 shows the location from where the samples were taken from the body of the CDPs and cut in the horizontal and vertical directions when filling the piece.

For grain size analysis, the surfaces of the cross-section of the samples were prepared with 2400 mesh sandpaper, without polishing, according to **Figure 9**, in sequence the samples were attacked for 15 seconds with Poulton's acid solution (60% HCL at 37%; 30% HNO₃ at 65%; 5% HF at 50% and 5% H₂O), then washed in water for 20 seconds. They were bleached with (67% HNO₃ at 65%, 5% HF at 50%, and 13% H₂O) and a time of 15 seconds. For the analysis of microstructural constituents, the cross-section surfaces, after prepared with 2400 mesh sandpaper, were polished with 1 μm alumina suspension and then chemically attacked with Keller reagent (95.0 ml distilled water, 2.5 ml HNO₃, 1.5 ml HCl and 1.0 ml HF).

The macro and microstructures were examined in an optical microscope with polarized light, filter plate, and differential interference contrast (DIC). The measurement of the average grain size (G) was conducted by the linear intercept method according to the ASTM E112-10 standard, 1996. The β-Fe intermetallic precipitate was analyzed by X-ray Dispersive Energy Spectroscopy (EDS) with the aid of a Tescan scanning electron microscope from Oxford Instruments to obtain the spatial spectra Al, Si, and Fe.

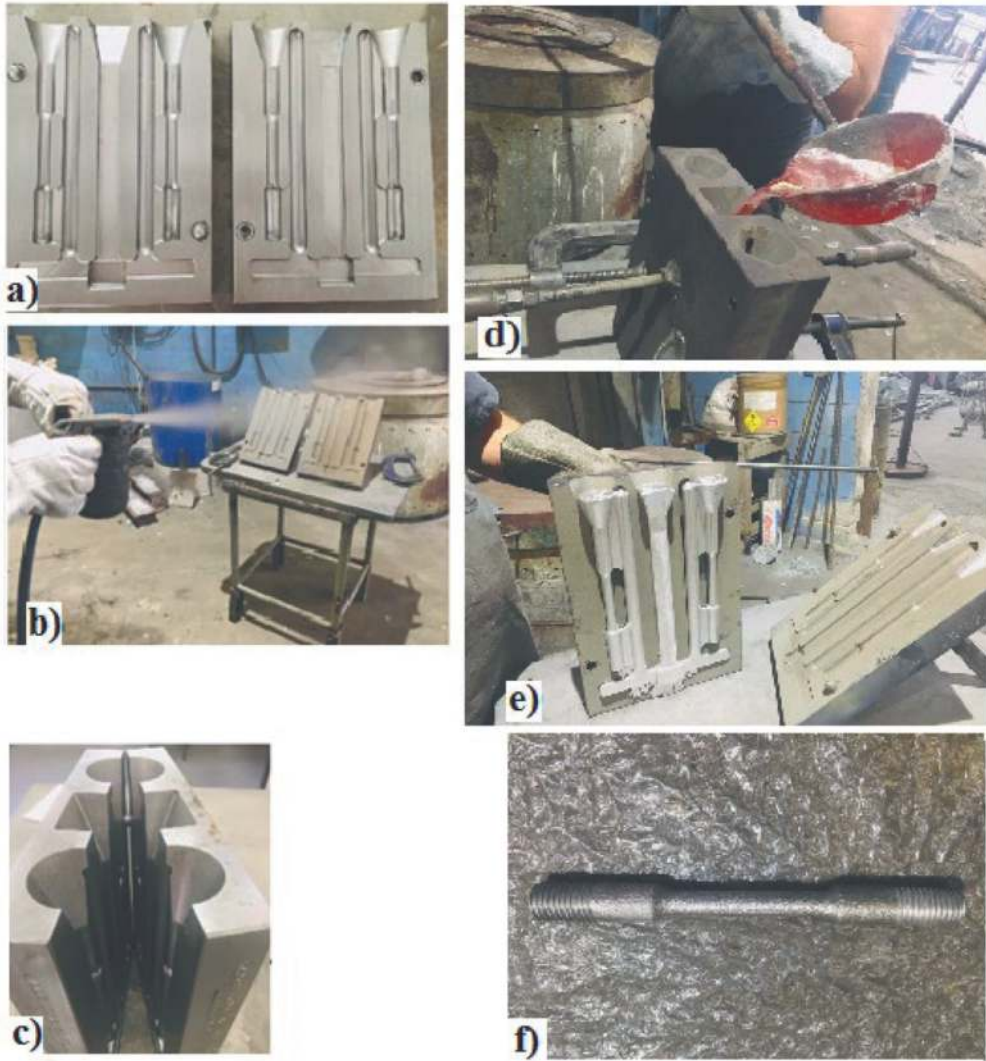


Figure 7. Leaking of the CPDs. a) Open mold. b) Painting the mold. c) Closing the mold. d) Leaking with manual transportation by ladle. e) Open mold with the CPD's. f) CPD without channels and massalots.

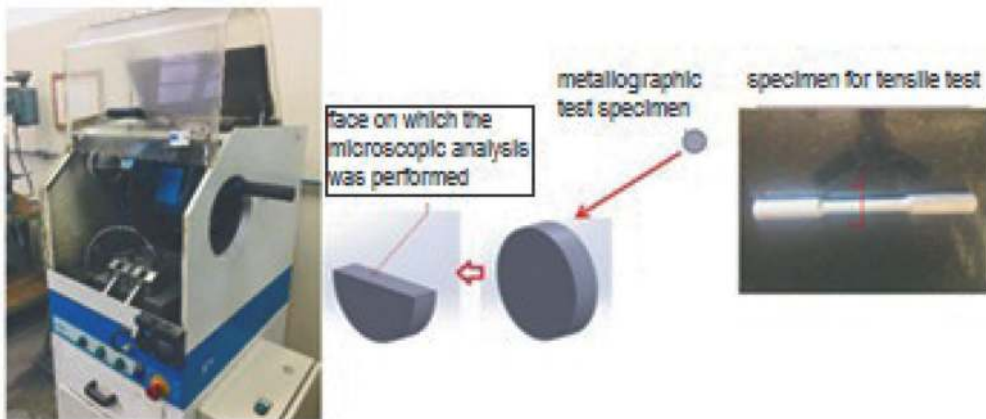


Figure 8. Cutting of the CPDs for sample preparation.



Figure 9.
Mounting, sanding, polishing, and finished sample.

2.3 Heat treatment

The heat treatment (T6) was performed in a Mufla furnace, OTTO WOLPERT - WERKE, located in the Metallurgy Laboratory of ITA. The parameters of heat treatment used were: temperature of $525 \pm 5^\circ\text{C}$, time of $4 \text{ h} \pm 15'$ (solubilization), immediately transferred to a water tank at room temperature (25°C) for 15 minutes (quenching). Subsequently, the CDPs were heated at a temperature of $175 \pm 5^\circ\text{C}$, time of $7 \text{ h} \pm 15'$ (precipitation or artificial aging), with subsequent cooling in the open air, as shown in **Figure 10**.

2.4 Tensile test

The tensile test was performed in a universal machine (brand Quanteq), model Emic Trd28 and equipped with a TestScript304 software for testing methods, located in the metallurgy laboratory of the Federal Institute of São Paulo (IFSP) - Campus Itaquaquecetuba, as shown in **Figure 11**. Data on yield stress, maximum stress, and material elasticity were obtained in the tests. Five CDPs were tested for each batch of material (**Table 1**), with and without T6.

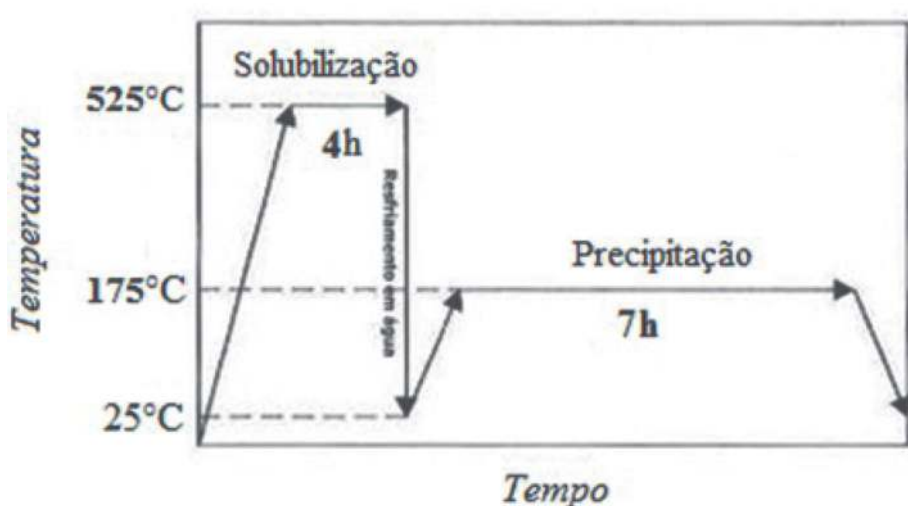


Figure 10.
Solubilization treatment followed by rapid cooling and precipitation.

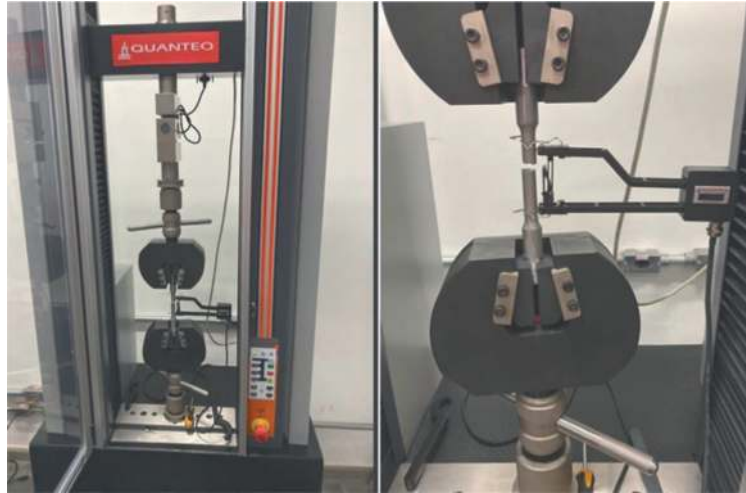


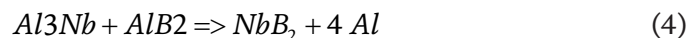
Figure 11.
Tensile test of sample $Al_{10}Si_1Fe$ with the addition of the inoculant $Nb + B$.

3. Results and discussion

In **Figure 12**, the microstructural analyses of the material revealed a drastic reduction in the grain size of the samples without and with the addition of the $Nb + B$ inoculant.

Highlighted in white outlines the dendrites without and with the addition of the inoculant $Nb + B$. The average grain size was calculated according to the linear intercept method. Overall, the reduction in the average grain size was 656% compared to the base alloys without the inoculant addition (from $787 \mu m$ to $120 \mu m$).

This transformation was due to the underlying mechanism of heterogeneous nucleation of clusters of Nb aluminum niobite substrates (Al_3Nb) and Nb niobium borides (NbB_2). These substrates were found in the core of $\alpha-Al$ grains, as shown in **Figure 13**. The heterogeneous transformation mechanism is also demonstrated in the literature and presented as shown in Eqs. (1) and (2) [24].



With the microstructural analyses, one can also identify the drastic change in the morphology of the $\beta-Fe$ particles. **Figure 14** shows by SEM images of the spectra of $\beta-Fe$ highlighted by light gray color, being in the samples without addition of the inoculant of elongated shape, **Figure 14(a)** and **(b)** and with the addition of 0.05% of $Nb + B$ with reduced size and spheroidised shape, **Figure 14(c)** and **(d)**.

The analysis of **Figure 14** shows the drastic reduction in the size and morphology of the $\beta-Fe$ intermetallic precipitates. Practically, the extinction of microporosity points, which are extremely harmful to the material, are crack initiation points when the material is subjected to mechanical stress. It is worth mentioning that this drastic reduction in the size of the intermetallic precipitate structures was achieved with a slow cooling rate. With this condition, it is very difficult to obtain the 'modification' of the needle-shaped eutectic phase and thick plate-shaped intermetallic precipitates

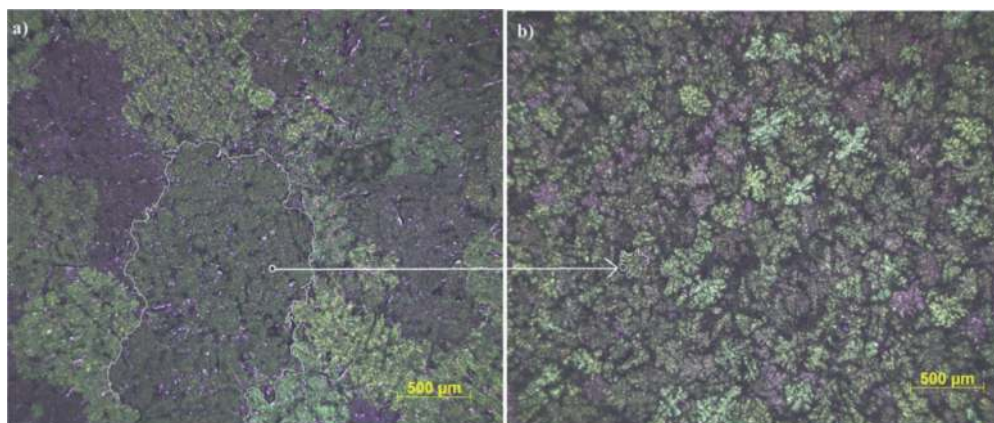


Figure 12.
Al₁₀Si₁Fe alloy, a) without inoculant and b) with Nb + B inoculant.

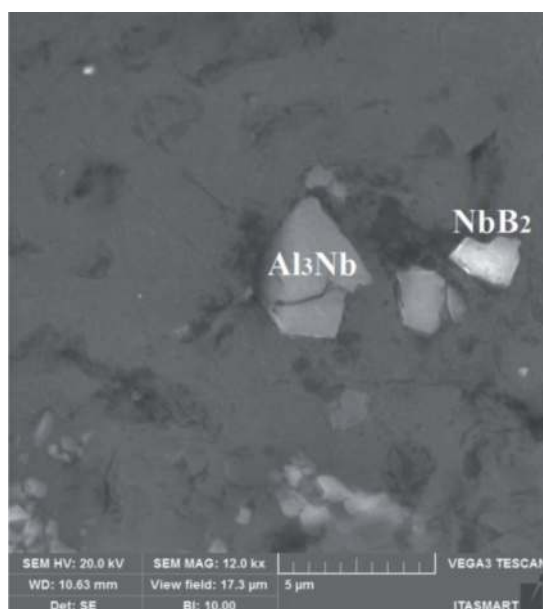


Figure 13.
Aluminum niobide substrates of (Al₃Nb) and niobium borides (NbB₂).

to morphology with reduced shape and size and spheroidized. This condition is highly desirable in the structure of the material.

After heat treatment (T6), the CDPs were tested in a universal traction machine under the conditions studied, as shown in **Table 1**. The results were tabulated, and the mean values of each sample were shown in the graph with the stress–strain curves, as shown in **Table 2** and **Figure 15**. Each color represents a test condition, as follows:

Red: samples with the base material.

Lilac: samples without the inoculant Nb + B, with Mg and heat treatment.

Green: samples with the addition of the inoculant Nb + B, without adding the element Mg and without heat treatment.

Blue: samples with the addition of the inoculant Nb + B, without adding the element Mg and with heat treatment.

Gray: samples with the inoculant Nb + B, with Mg and heat treatment.

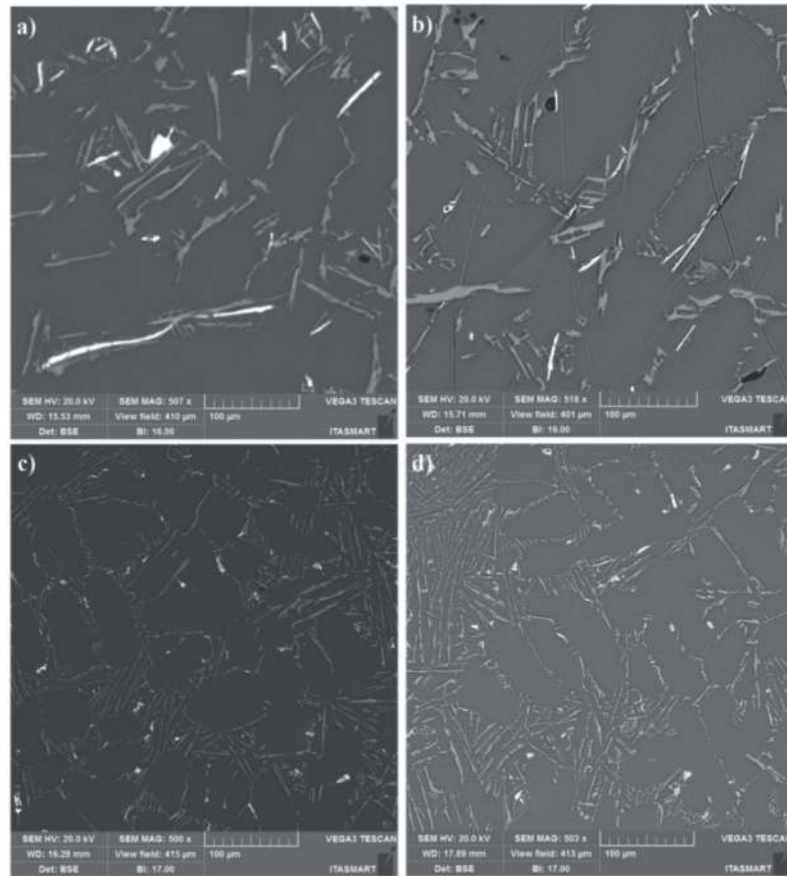


Figure 14. Image with 500X magnification, showing the morphology of the β -Fe spectra in light gray color. (a, b) before addition of Nb + B; (c, d) after addition of Nb + B.

Propriedades mecânicas			
	Tensão de escoamento (MPa)	Tensão máxima (MPa)	Elasticidade (%)
	95.5	197	2.12
	143	191	2.60
	194	261	2.02
	77.5	194	7.56
	208	300	4.66

Table 2. Mechanical properties for each sample condition studied.

When we compared the red curve with the purple curve, the results were: gain of 50% in the yield strength (from 95.5 MPa to 143 MPa), without a gain in the strength limit (from 197 MPa to 191 MPa), with little evolution regarding the percentage elongation (from 2.12% to 2.60%). In the alloy without the addition of the inoculant Nb + B, the precipitates of β -Fe coming from the Fe-critical in the alloy present with morphology in the form of plates or coarse needles, as shown in **Figure 14(a)** and **(b)**, which are generally not affected by the typical T6 heat-treatment process. In the alloy

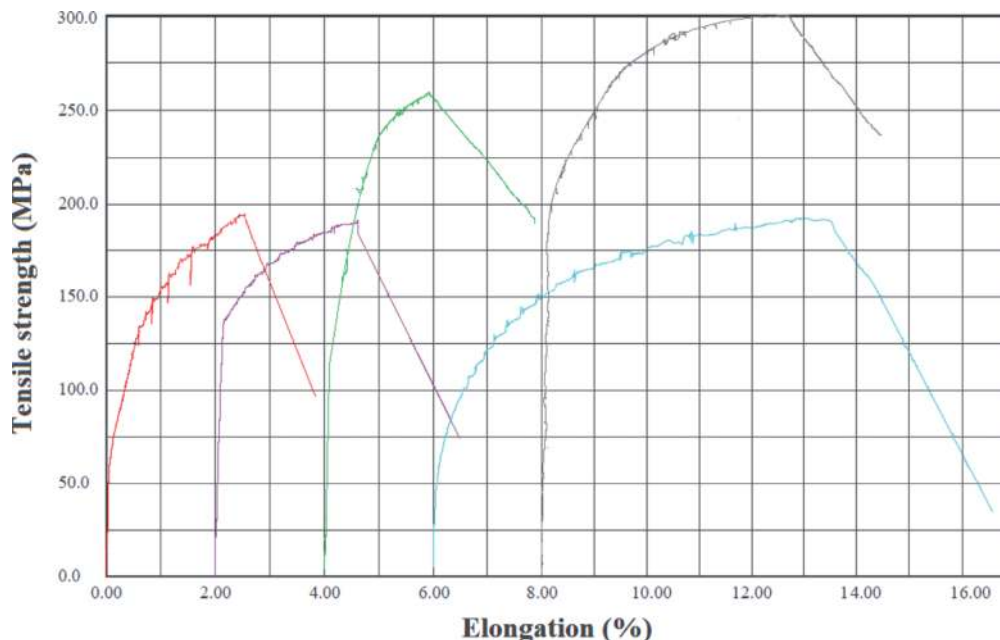


Figure 15.

A resistência à tração em função do alongamento Para os lotes fundidos. Material base (curva vermelha); com adição do elemento Mg e tratamento térmico (curva lilás); com adição de Nb + B e sem tratamento térmico (curva verde); com adição de Nb + B e com tratamento térmico (curva Azul); com adição de Nb + B, o elemento Mg e T6 (curva cinza).

with Mg, Mg_2Al_3 precipitates are formed, solubilized, and precipitated in finely dispersed particles during the T6 heat treatment, serving as a reinforcement mechanism for the material in its elastic region, which justifies the increase in elasticity found. On the other hand, in the plastic region, with the increase in stress, the β -Fe particles are like rigid points in the material's structure. They did not deform, initiating cracks, which ended up embrittling and limiting the maximum strength of the material. Signaling that the effect of heat treatment is not beneficial in alloys with Fe-critical.

When we compare the red curve with the green curve, the results were: gain of 203% in the yield strength (from 95.5 MPa to 194 MPa), a gain of 32.5 in the resistance limit (from 197 MPa to 261 MPa). However, without evolution as for the percentual elongation (from 2.12% to 2.02%). The reduced grains due to the inoculation via Nb + B brought greater grain contours. The grain contours are discontinuities that hinder the movement of discordances, improving the strength of the material. The α -Al grain inoculation via Nb + B caused a casting structure with equiaxial and reduced grain size and a structure without coarse plates of β -Fe particles and no presence of micro porosities, as verified in **Figure 14(c)** and **(d)**. However, the smaller and stiffer grains ended up reducing the elongation of the material, being below the reference value of the base alloy. Signaling that only the addition of the inoculant Nb + B was not enough to achieve the desired elongation to the material with Fe-critical.

When we compared the red curve with the blue curve, the mechanical behavior regarding the percentage elongation was transformed. The gain was 357% (from 2.12% to 7.56%). However, there was a reduction in the yield strength (from 95.50 MPa to 77.5 MPa) and no evolution in the strength limit of the material (from 197 MPa to 194 MPa). Due to the heat treatment, solubilization, the α -Al grain size was reconstituted. The plastic deformation started at a lower stress plateau but extended until

about 7.6% strain. The material's behavior regarding the strength limit remained similar to that of the base material. Similar to the previous discussion, the material without the coarse plates formed by the β -Fe particles and without the presence of micro porosities improved its ductility, presenting a higher plastic deformation than the other conditions, with the retardation of the crack points, promoting a continued strain hardening until reaching the maximum stress during the plastic deformation. Although these characteristics are interesting for some mechanical applications, the addition of Nb + B, with subsequent T6 heat treatment, did not affect raising the desired strength levels without the addition of the Mg element.

The Mg element was introduced, and the aging treatment was carried out to achieve higher strength levels.

With the addition of the element Mg in the alloy refined with Nb + B and after the heat treatment of solubilization and precipitation T6 (gray curve), there were gains in tensile strength and elasticity levels when compared to the base alloy. Regarding the elongation, there was a gain of 90% compared to the alloy base material (from 2.12% to 4.66%), in the yield strength, the gain was 217.5% (from 95.5 MPa to 208 MPa), and in the tensile strength, the gain was 53% (from 197 MPa to 300 MPa).

It is interesting to note that only introducing the Mg element and the aging precipitation treatment (T6) increase the yield strength. Still, it is not efficient to raise the strength limit or ductility of the alloy. The introduction of only Nb + B as inoculant significantly increases the yield strength, raises the strength limit, but there is a 5% loss in elongation. When applying to this alloy, which received only the inoculant Nb + B, the aging treatment significantly increases the elongation (357%) but with loss in yield strength. The best combination of properties was observed when, in addition to the inoculant Nb + B, the element Mg was incorporated into the alloy. The aging treatment was performed (T6). In this case, there was an increase in yield strength (217.5%) in the strength limit (53%) and elasticity, measured by elongation (90%).

4. Conclusions

The addition of the inoculant Nb + B is a powerful tool for the primary α -Al grain refinement in AlSi alloys with critical Fe.

The refinement of the α -Al grain from the proposed inoculant (Nb + B) significantly changed the morphology and size of β -Fe precipitates, making them reduced and spheroidized.

In the Al10Si1Fe cast alloy, inoculated with 0.05% Nb and 0.063% B, with aging (T6) and without introducing the Mg element, there is a large gain in elongation (357%), but without gains in mechanical strength.

In the Al10Si1Fe cast alloy, inoculated with 0.05% Nb and 0.063% B, with aging (T6) and with the introduction of the Mg element, it was the best condition of the mechanical property achieved, with an increase in yield strength (217.5%), strength (53%) and elasticity, measured by elongation (90%).

The refinement promoted by the addition of Nb + B inoculant did not change the precipitation hardening mechanism of Mg₂Al₃. Similarly, the reconstitution of the α -Al grain size promoted during the solubilization of the material did not alter the morphology of the reduced and spheroidised β -Fe particles.

The beneficial actions of the two techniques used for strengthening the material's mechanical properties added up, providing strength and elasticity to the material, properties that are sought after in engineering applications.

The mechanical properties obtained with the studied alloy suggest using alloys coming from recycling (Fe-Critical) in engineering applications with structural and safety parts.

Acknowledgements

The author would like to thank CAPES (Coordenação de Aperfeiçoamento de Pessoal de Nível Superior) - funding code 001, for providing financial support for this study. The author is also grateful to the Institute of Aeronautical Technology, the Institute of Advanced Studies, and the Federal Institute of Education, Science and Technology of São Paulo (IFSP) - Itaquaquecetuba campus for the practice and support very kindly provided.

Conflict of interest

The authors declare no conflict of interest.

Notes/thanks/other declarations

Thanks to the teacher Dr. A. J. Abdalla, for every support during this research.

Author details

Narducci Carlos Jr.^{1,2,3}


1 Aeronautics Institute of Technology – ITA, São José dos Campos, Brazil

2 Institute for Advanced Studies – IEAv, São José dos Campos, Brazil

3 Federal Institute of São Paulo – IFSP, Itaquaquecetuba, Brazil

*Address all correspondence to: cnarducci@ifsp.edu.br

IntechOpen

© 2021 The Author(s). Licensee IntechOpen. This chapter is distributed under the terms of the Creative Commons Attribution License (<http://creativecommons.org/licenses/by/3.0>), which permits unrestricted use, distribution, and reproduction in any medium, provided the original work is properly cited. 

References

- [1] GREEN J.A.S. Aluminum Recycling and Processing for Energy Conservation and Sustainability; ASM International Materials Park, Ohio 44073-0002; US, 2007.
- [2] MACHADO, C. T. S. et. al. A reciclagem de alumínio como vantagem estratégica de negócios em uma indústria metalúrgica. estudo de caso; XI INC; XI EPG; Universidade do Vale do Paraíba - 2011.
- [3] TAYLOR, J. A; Iron-containing intermetallic phases in Al-Si based casting Alloys. ELSEVIER, Procedia Materials Science 1 19 – 33, Australia, 2012. CALLISTER, W. D. J. Fundamentos da Ciência e Engenharia de Materiais. 2ª Ed. LTC. Brasil, R. J. 2005.
- [4] PORTER, D. A. EASTERLING, K. E. Phase transformations metals and alloys. Chapman Halls. Van Nostrand Reinhold Co., UK, London, 1981.
- [5] SHEWMON, P.G. Transformations in metals, McGrawHill. New York, 1969.
- [6] REED-HILL, R. E. Princípios de Metalurgia Física. Second Edition; Editora Guanabara. R.J, 1982.
- [7] CALLISTER, W. D. J. Fundamentos da Ciência e Engenharia de Materiais. 2ª Ed. LTC. Brasil, R. J. 2005.
- [8] TURNBULL, D. FISHER, J. C. Journal of Chemical Physic. 17.71 (1948): 71-73. 1948.
- [9] JACKSON K, A. HUNT, J. P. Acta Met. 13(1965): 1212. 1965.
- [10] TRIVERDI, R. KURZ, W. Int. Mat. Rev. 39 (1994): 129. 1994.
- [11] BRUNATTO, S. F. Ligas Metálicas e Diagramas de Fases. INTMAT-2, GTFAP&MP, CNPQ. São Paulo, 2012.
- [12] MARK, E. DAVID, ST. J. Grain Refinement of Aluminum Alloy: Part I. The Nucleant and Solute paradigms – A Review of the Literature. Metallurgical and materials Transactions. Jun 1999; 30A, 6; Academic Research library, pg 1613. Australia, 1999.
- [13] MARK, E. DAVID, ST. J. Grain Refinement of Aluminum Alloy: Part II. Confirmation of, and a mechanism for, the Solute paradigms. Metallurgical and materials Transactions. Jun 1999; 30A, 6; Academic Research library, pg 1625. Australia, 1999.
- [14] NARDUCCI, C. J. BROLLO, G. L. SIQUEIRA, R. H. M. ANTUNES, A. S. ABDALLA, A. J. Effect of Nb addition on the size and morphology of the β -Fe precipitates in recycled Al-Si alloys; Scientific Reports, Springer Nature. <https://doi.org/10.1038/s41598-021-89050-5>. Brazil, SP, 2021.
- [15] NOWAK, M. BOLZONI, L. BABU, N. H. Grain refinement of Al-Si alloys by Nb-B inoculation. Part I. Materials and Desigs. 66 (2015) 366-375. UK, 2015.
- [16] BOLZONI, L. NOWAK, M. HARI BABU, N. Grain refinement of Al-Si alloys by Nb-B inoculation. Part II: Application to commercial alloys. Materials and Design. 66 (2015) 376-383, 2015. UK, 2015.
- [17] XU J, LI R, LI Q. Effect of Agglomeration on Nucleation Potency of Inoculant Particles in the Al-Nb-B Master Alloy: Modeling and Experiments[J]. Metallurgical and Materials Transactions A. 2021: 1-18. China, 2021.

[18] APELIAN, D. Aluminum Cast Alloys: Enabling Tools for Improved Performance. Wheeling: North American Die Casting Association. USA, 2009.

[19] MCQUEEN, J. H. SPIGARELLI, S. KASSNER, M. E. EVANGELISTA E. Hot Deformation and Processing of Aluminum Alloys. CRC Press. USA - NW, 2011.

[20] VERRAN, E. H. BATISTA, G. M. Análise dos efeitos dos tratamentos térmicos de solubilização e envelhecimento artificial sobre a microestrutura da liga de alumínio; Matéria R. J. Brasil, Rio de Janeiro, 2015.

[21] CAVALCANTE, F.F. Comportamento mecânico e tenacidade à fratura de ligas de alumínio: 2024 e 7075, submetida a diferentes tempos de envelhecimento. Dissertação, Engenharia dos materiais, UFRN. Brasil, RN, 2016.

[22] SHAKELFORD, J. F. Introdução a ciências dos materiais para engenheiros. PEARSON, 6ª ed., USA, 2008.

[23] BOLZONI, L. HARI BABU, N. Towards industrial Al-Nb-B master alloys for grain refining Al-Si alloys. J Materiores Technol . 2019; 8(6): 5631-5638, 2019.

[24] BOLZONI, L. BABU, N. H. Engineering the heterogeneous nuclei in Al-Si alloys for solidification control. Materials Today 5 (2016) 255-259. UK, November 2016.